S & M 1851

Luminescence and Scintillation Properties of Eu-doped $CaAl_2O_4$ Bulk Crystals

Daisuke Nakauchi,[1*] Noriaki Kawaguchi,[1] and Takayuki Yanagida[1]

[1]Division of Materials Science, Nara Institute of Science and Technology (NAIST),
8916-5 Takayama, Ikoma, Nara 630-0192, Japan

(Received November 30, 2018; accepted March 25, 2019)

Keywords: scintillator, dosimetry, photoluminescence, radioluminescence, crystal growth, afterglow

Eu-doped $CaAl_2O_4$ bulk crystals were synthesized by the floating zone (FZ) method, and their photoluminescence (PL) and scintillation properties were investigated firstly in a bulk crystal. The crystal samples exhibit PL and radioluminescence (RL) with a broad emission peaking around 440 nm as well as sharp peaks appearing around 600 nm, which are similarly observed for powder samples. Suggested from the decay time constants, they are attributed to the 5d–4f transitions of Eu^{2+} and the 4f–4f transitions of Eu^{3+}, respectively. From the pulse height spectrum under ^{241}Am γ-ray (59.5 keV) exposure, the light yield (LY) of a 3.0% Eu:$CaAl_2O_4$ bulk crystal is approximately 12000 ph/MeV.

1. Introduction

Scintillators utilizing inorganic luminescent materials have a function to immediately convert ionizing radiation into low-energy photons, so they have been attracting considerable interest in response to increasing demands of radiation detection including medical imaging,[(1)] security,[(2)] astrophysics,[(3)] environmental monitoring,[(4)] and resource exploration, e.g., oil-dwelling.[(5)] In recent years, a divalent europium (Eu^{2+}) center has attracted attention as a luminescent center of scintillators. Eu^{2+} shows the luminescence due to the spin- and parity-allowed 5d–4f transitions with a broad absorption and emission band in ultraviolet and visible regions.[(6)] Since Eu^{2+} exhibits a relatively short decay time and a high emission efficiency, Eu^{2+}-doped scintillators with a high sensitivity to various types of ionizing radiation have been developed.[(7–9)] The luminescence of Eu^{2+}, originating from the $4f^7 \rightarrow 4f^6 5d$ transition, strongly relies on the type of environment (e.g., crystal field) around Eu^{2+} ions. This means that the emission wavelength of a Eu-doped scintillator depends on the host material. Therefore, from an academic viewpoint, the investigation of new Eu-doped materials is very interesting.

Alkaline-earth aluminates have been our recent interest for scintillator applications.[(10–14)] Over the past decades, Eu^{2+}-doped alkaline-earth aluminates have been widely studied as phosphors with a bright luminescence in the visible wavelength range.[(15–17)] In particular, Nd-Eu-codoped calcium dialuminate ($CaAl_2O_4$), which is discovered by Yamamoto and

*Corresponding author: e-mail: nakauchi.daisuke.mv7@ms.naist.jp
https://doi.org/10.18494/SAM.2019.2184

ISSN 0914-4935
https://myukk.org/

Matsuzawa,[18] is known as the most famous blue persistent phosphor showing a long-lasting luminescence.[19,20] However, in spite of the great luminescence properties,[21,22] no study has been reported on the observation of radioluminescence (RL) from Eu:$CaAl_2O_4$ as far as we know. Previously, we showed that a Eu-doped $SrAl_2O_4$ bulk crystal, which belongs to the alkaline-earth aluminate group as well, exhibits a notably high scintillation light yield (LY).[11] Therefore, Eu:$CaAl_2O_4$ is also a promising candidate for scintillators.

In this study, Eu:$CaAl_2O_4$ bulk crystals with various Eu concentrations were synthesized by the floating zone (FZ) method and characterized to exhibit photoluminescence (PL) and scintillation properties. Although $CaAl_2O_4$ is composed of light elements and may not be ideal as general scintillators for X- or γ-ray detections, it can be used for particle detectors such as Ce:YAG and Ag:ZnS.[23]

2. Materials and Methods

Eu-doped $CaAl_2O_4$ crystals were synthesized using an FZ furnace (FZD0192, Canon Machinery). First, Eu_2O_3 (99.99%), CaO (99.99%), and Al_2O_3 (99.99%) powders were mixed with a molar ratio of Eu_2O_3:CaO:Al_2O_3 = x/2:100 − x:100 (x = 1, 2, 3, and 5). Then, the homogenously mixed powder was formed into a cylinder rod by applying hydrostatic pressure to the mixture powder loaded in a cylindrical balloon. Next, the rod was sintered at 1250 ℃ for 6 h in air to obtain a polycrystalline rod. The sintered rod was loaded into the FZ furnace, and crystal growth was induced at a rotation rate of 20 rpm and a pull-down rate of 5 mm/h. Here, the heating source of the FZ furnace was a halogen lamp. To identify the obtained crystalline phases, the powder X-ray diffraction (XRD) pattern was measured using a diffractometer (MiniFlex600, Rigaku) over the 2θ range of 5–90°. The X-ray source is a conventional X-ray tube with a CuKα target operated at 40 kV and 15 mA.

The PL quantum yield (QY) as well as PL excitation (PLE) and PL contour plots were measured using a Quantaurus-QY (Hamamatsu Photonics, C11347-01). The PLE spectrum was obtained using a spectrofluorometer (FP8600, JASCO). The PL decay time profile was evaluated using a Quantaurus-τ (Hamamatsu Photonics, C11367), where the monitoring wavelengths were 440 and 610 nm. As scintillation properties, the X-ray-induced RL spectrum was measured utilizing our original setup.[24] The X-ray generator (Spellman, XRB80P&N200X4550) was equipped with an ordinary X-ray tube having a tungsten anode target and a beryllium window. The X-ray tube was operated with a bias voltage of 40 kV and a tube current of 5.2 mA. The emitted RL photons were guided to a spectrometer (Andor DU-420-BU2 CCD with a Shamrock SR163 monochromator) through an optical fiber of 2 m length. The detector was cooled to 188 K by using a Peltier module to reduce the thermal noise. Furthermore, the RL decay time and afterglow profiles were measured using an afterglow characterization system equipped with a pulsed X-ray tube.[25] The sensitivity of the photomultiplier tube (PMT) used is in the measurement range from 160 to 650 nm. For both PL and RL decay time profiles, the decay time constant (τ) was deduced by least-squares fitting with an exponential decay function. For pulse height spectrum measurements, a sample was mounted on the window of the PMT (Hamamatsu Photonics, R7600-200) with silicon grease

(OKEN, 6262A), and the sample was covered with several layers of Teflon reflectors to guide the RL photons to the PMT. The RL photons were converted to an electrical signal, which was then processed using a preamplifier (ORTEC, 113), a shaping amplifier (ORTEC, 570), and a multichannel analyzer (Amptek, Pocket MCA 8000A). The pulse height spectrum was eventually stored in a computer. Here, the shaping times were 2 μs for Eu:$CaAl_2O_4$ samples and 0.5 μs for the reference Ce:Gd_2SiO_5 sample.

Figure 1 shows photographs of the synthesized Eu:$CaAl_2O_4$ crystals. The samples look colorless and transluscent. The typical size was 4–5 mmϕ × 10–20 mm. Under ultraviolet light (254 nm), a bright blue emission was seen by the naked eyes. The crystalline rods were cut into small pieces to characterize the luminescence properties of the crystals.

Figure 2 shows powder XRD patterns of the Eu:$CaAl_2O_4$ crystals and Crystallography Open Database information card (COD-2002888) for comparison. The reference XRD patterns are in agreement with the XRD patterns of all the samples, which demonstrate diffraction peaks of a $CaAl_2O_4$ single phase. The XRD patterns showed that the obtained materials belong to the $P\ 1\ 2_1/n\ 1$ space group of the monoclinic crystal system, and no impurity phases can be observed.

Figure 3(a) shows the PLE-PL contour plot of the 5.0% Eu:$CaAl_2O_4$ crystal. In spite of Eu concentrations, all the samples exhibit a PL emission with a broad band around 440 nm as well as sharp signals around 570–700 nm. The broad emission is due to the 5d–4f transitions of Eu^{2+}, while the sharp signals are due to the 4f–4f transitions of Eu^{3+} ($^5D_0 \rightarrow {}^7F_J$, $J = 0$–4). Here, the spectral shape of the broad emission is affected by the absorption peak at 460 nm due to Eu^{3+} ($^7F_0 \rightarrow {}^5D_2$)[26] as shown in Fig. 3(b). The internal PL QYs of the 1.0, 2.0, 3.0, and 5.0% Eu-doped samples are 6.8, 13.7, 19.0, and 18.4%, respectively. Among the synthesized samples, the 3.0% Eu-doped crystal sample exhibits the highest QY; however, the value is lower than that of a Eu:$SrAl_2O_4$ crystal (~50%[11]).

As presented in Fig. 4, the PL decay time profiles are monitored at 440 nm. The decay curve is well approximated using a single exponential decay function, and the obtained decay time constants are about 160–180 ns. From the obtained decay time constants, the fast component is due to the 5d–4f transitions of Eu^{2+}.[27] Figure 5 shows the decay time profiles monitored at

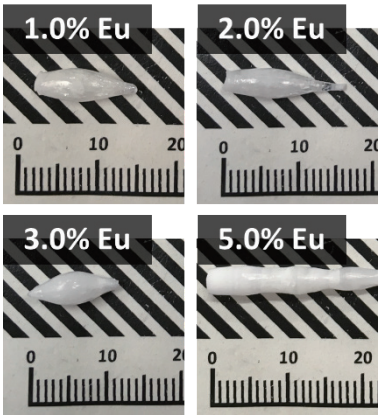

Fig. 1. (Color online) Photographs of Eu:$CaAl_2O_4$ crystals.

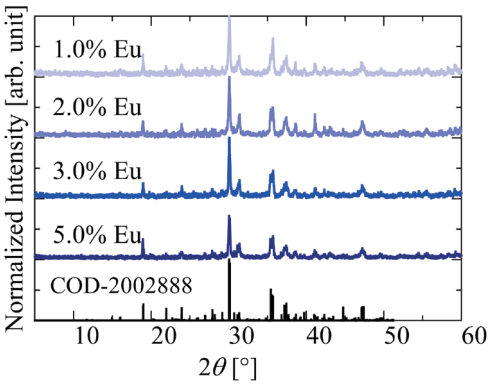

Fig. 2. (Color online) Powder XRD patterns of synthesized Eu:$CaAl_2O_4$.

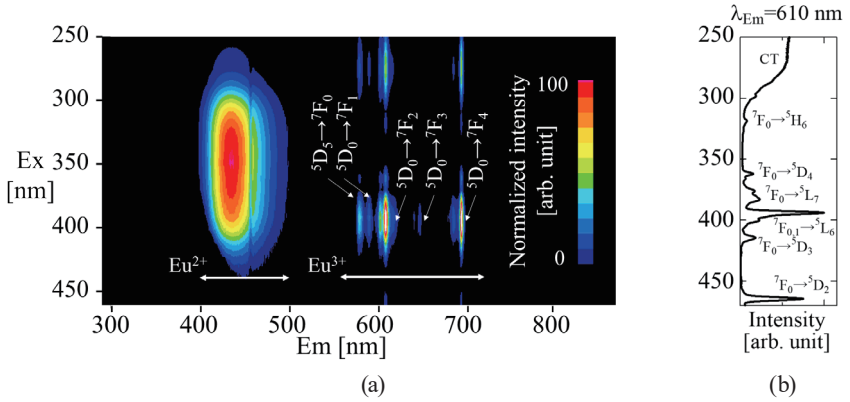

Fig. 3. (Color online) (a) Representative PLE-PL contour plot of a 5.0% Eu:$CaAl_2O_4$ crystal and (b) a PLE spectrum monitored at 610 nm.

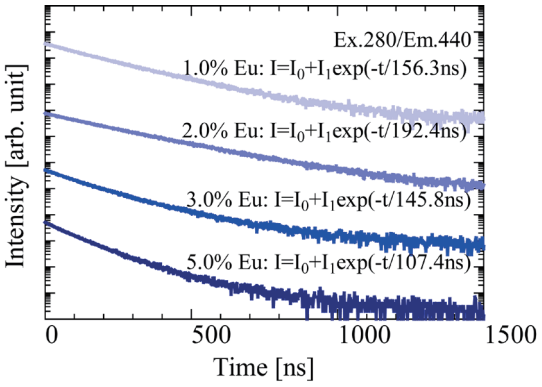

Fig. 4. (Color online) PL decay curves of Eu:$CaAl_2O_4$ crystals with different Eu concentrations. The PL decay signals were monitored at 440 nm at an excitation wavelength of 280 nm.

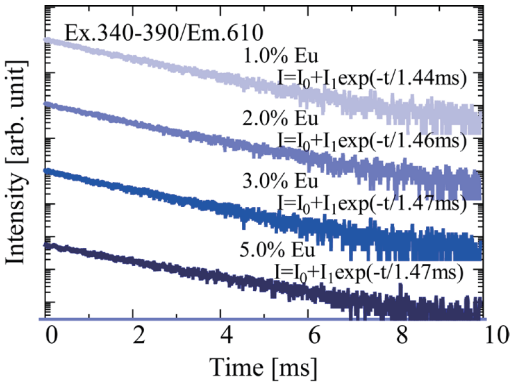

Fig. 5. (Color online) PL decay curves of Eu:$CaAl_2O_4$ crystals with different Eu concentrations. PL decay signals were monitored at 610 nm at an excitation wavelength of 340–390 nm.

610 nm. The decay time curves are also composed of an exponential function, where the decay time constants are close to the typical decay time constant of the 4f–4f transitions of Eu^{3+}.[28,29]

Figure 6 shows the X-ray-induced RL spectra. The Eu:$CaAl_2O_4$ crystals show RL predominantly with a broad emission band peaking around 440 nm as well as weak peaks around 600 nm. Also, in the case of in PL, the broad emission is attributed to the 5d–4f transitions of Eu^{2+}, while the weak peaks seem to be due to the 4f–4f transitions of Eu^{3+} ($^5D_0 \rightarrow {}^7F_J$, J = 0–4). The inset table in Fig. 6 shows the ratio of integral values of Eu^{3+} and Eu^{2+} emissions. As the Eu concentrations increases, the Eu^{3+} emission peaks around 600 nm as well as absorption signals at 460 nm appear to increase. Although the sample sizes are not exactly the same, it seems that the 3.0% Eu-doped sample shows the highest RL intensity of the broad emission among the samples. Figure 7 shows the X-ray-induced RL decay time profiles measured in the nanosecond range. The curves were approximated using a sum of two exponential decay functions. The decay time constants of fast components are 30–40 ns, while those of slow components, which account for ~90%, are 100–200 ns. Suggested from the decay

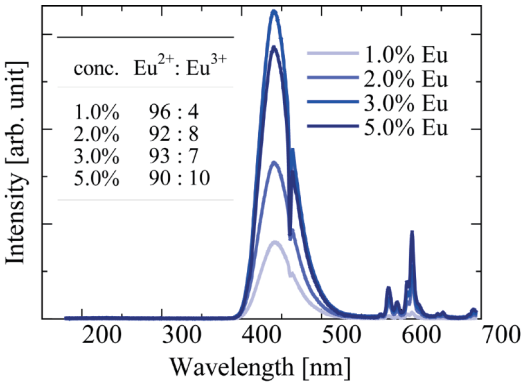

Fig. 6. (Color online) X-ray-induced RL spectra. The inset table shows the ratio of integral values of Eu^{3+} and Eu^{2+} emissions.

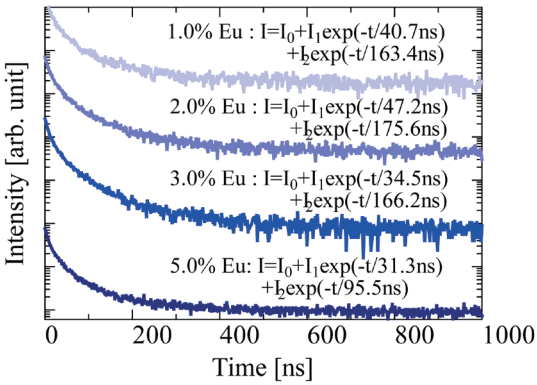

Fig. 7. (Color online) X-ray-induced RL decay curves. The wavelength sensitivity of the PMT ranges from 160 to 650 nm.

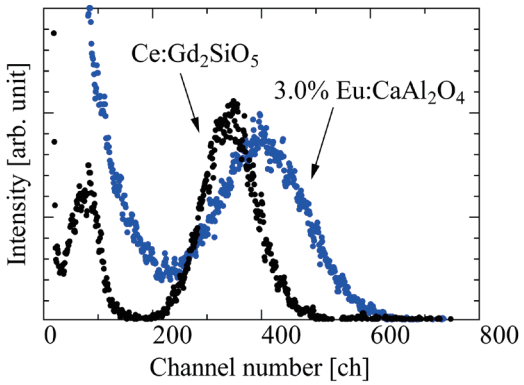

Fig. 8. (Color online) Pulse height spectra measured using 3.0% Eu:$CaAl_2O_4$ crystal and Ce:GSO under ^{241}Am γ-ray exposure.

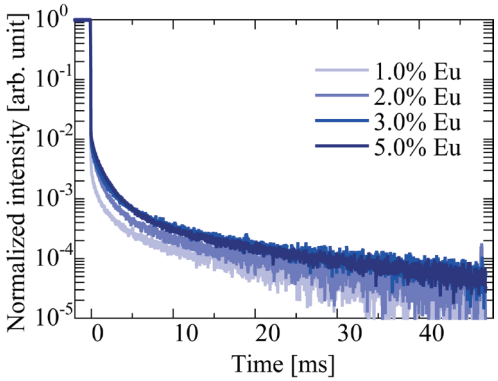

Fig. 9. (Color online) Afterglow curves of Eu:$CaAl_2O_4$ crystals after 2 ms X-ray exposure.

time constants, the origins are some lattice defects in the host and the 5d–4f transitions of Eu^{2+}, respectively. The decay time constants of the Eu^{2+} emission are similar to those of PL and smaller than those of Eu:$SrAl_2O_4$ crystals.[11]

Figure 8 shows the pulse height spectrum measured using the 3.0% Eu:$CaAl_2O_4$ crystal under ^{241}Am gamma-ray (59.5 keV) exposure. The pulse height spectrum was also measured using a Ce:GSO single crystalline scintillator as a reference, which has a broad emission peaking around 430 nm and a scintillation LY of 10000 photons/MeV.[30] The 3.0% Eu-doped sample exhibits a clear photoabsorption peak, while the rest do not. From the photoabsorption peak channel, the scintillation LY of the sample is 12000 photons/MeV with a typical error of ±10%. Although the LY of the Eu:$CaAl_2O_4$ crystal is lower than those of Eu:$SrAl_2O_4$ crystals [11] as well as the famous scintillators consisting of light elements such as Ce:YAG, the emission wavelengths are more suitable for common PMTs with high quantum efficiency in the blue region.[31]

The afterglow curves of the synthesized samples after 2 ms X-ray exposure are shown in Fig. 9. In the analyses of the curves, the afterglow level (A) is defined as $A = 100 \times (I_2 - I_{BG})/(I_1 - I_{BG})$.

Here, I_{BG}, I_1, and I_2 denote the mean signal intensity before X-ray exposure, the mean signal intensity during X-ray exposure, and the signal intensity at t = 20 ms after X-ray irradiation, respectively. The calculated afterglow levels are 74 (1.0%), 99 (2.0%), 163 (3.0%), and 150 ppm (5.0%). The obtained afterglow levels of the Eu:$CaAl_2O_4$ crystals are ten times as high as those of practical scintillators (~10 ppm).[25] Among the present samples, the 1.0% Eu-doped crystal shows the lowest afterglow level.

3. Conclusions

Eu-doped $CaAl_2O_4$ crystals were synthesized by the FZ method. The obtained crystals exhibit PL and RL with a broad emission band around 440 nm due to the 5d–4f transitions of Eu^{2+} as well as several sharp peaks due to the 4f–4f transitions of Eu^{3+}. The decay time constants are the typical values of each origin. From pulse height spectra under ^{241}Am γ-ray (59.5 keV) exposure, the LY of the 3.0% Eu-doped $CaAl_2O_4$ crystal is estimated to be approximately 12000 photons/MeV. The Eu-doped $CaAl_2O_4$ crystals can be a new scintillation candidate showing a blue emission suitable for sensitivity wavelengths of common PMTs. However, Eu-doped $CaAl_2O_4$ crystals have relatively high afterglow signals, which are unacceptable in integrated applications. To expand the scope of application, further study is required.

Acknowledgments

This work was supported by Grants-in-Aid for Scientific Research A (17H01375), Scientific Research B (18H03468), Early-Career Scientists (18K14158), JSPS Research Fellow (17J09488) from Japan Society for the Promotion of Science (JSPS), and A-STEP from Japan Science and Technology Agency (JST). The Cooperative Research Project of Research Institute of Electronics, Shizuoka University, KRF Foundation, Terumo Foundation for Life Sciences and Arts, Izumi Science and Technology Foundation, The Iwatani Naoji Foundation, The Kazuchika Okura Memorial Foundation, and NAIST Foundation are also acknowledged.

References

1 S. Yamamoto, S. Okumura, N. Kato, and J. Y. Yeom: J. Instrum. **10** (2015) T09002. https://doi.org/10.1088/1748-0221/10/09/T09002
2 J. Glodo, Y. Wang, R. Shawgo, C. Brecher, R. H. Hawrami, J. Tower, and K. S. Shah: Phys. Procedia **90** (2017) 285. https://doi.org/10.1016/j.phpro.2017.09.012
3 T. Itoh, T. Yanagida, M. Kokubun, M. Sato, R. Miyawaki, K. Makishima, T. Takashima, T. Tanaka, K. Nakazawa, T. Takahashi, N. Shimura, and H. Ishibashi: Nucl. Instrum. Methods Phys. Res., Sect. A **579** (2007) 239. https://doi.org/10.1016/j.nima.2007.04.144
4 L. Salonen: Sci. Total Environ. **130–131** (1993) 23. https://doi.org/10.1016/0048-9697(93)90056-C
5 C. L. Melcher: Nucl. Instrum. Methods Phys. Res., Sect. B **40**–**41** (1989) 1214. https://doi.org/10.1016/0168-583X(89)90622-8
6 P. Dorenbos: J. Phys. Condens. Matter **15** (2003) 2645. https://doi.org/10.1088/0953-8984/15/17/318
7 D. Nakauchi, G. Okada, N. Kawaguchi, and T. Yanagida: J. Mater. Sci. Mater. Electron. **28** (2017) 6972. https://doi.org/10.1007/s10854-016-5752-2
8 K. Watanabe, T. Yanagida, and K. Fukuda: Sens. Mater. **27** (2015) 269
9 N. J. Cherepy, G. Hull, A. D. Drobshoff, S. A. Payne, E. Van Loef, C. M. Wilson, K. S. Shah, U. N. Roy, A. Burger, L. A. Boatner, W. S. Choong, and W. W. Moses: Appl. Phys. Lett. **92** (2008) 1. https://doi.org/10.1063/1.2885728

10 D. Nakauchi, G. Okada, M. Koshimizu, and T. Yanagida: J. Rare Earths **34** (2016) 757. https://doi.org/10.1016/S1002-0721(16)60090-X
11 D. Nakauchi, G. Okada, M. Koshimizu, and T. Yanagida: J. Lumin. **176** (2016) 342. https://doi.org/10.1016/j.jlumin.2016.04.008
12 D. Nakauchi, G. Okada, M. Koshimizu, and T. Yanagida: Nucl. Instrum. Methods Phys. Res., Sect. B **377** (2016) 89. https://doi.org/10.1016/j.nimb.2016.04.017
13 D. Nakauchi, G. Okada, M. Koshimizu, and T. Yanagida: Radiat. Meas. **106** (2017) 170. https://doi.org/10.1016/j.radmeas.2017.03.021
14 D. Nakauchi, G. Okada, K. Masanori, N. Kawano, N. Kawaguchi, and T. Yanagida: Nucl. Instrum. Methods Phys. Res., Sect. B **435** (2018) 273. https://doi.org/10.1016/j.nimb.2018.01.007
15 S. H. M. Poort, W. P. Blokpoel, and G. Blasse: Chem. Mater. **7** (1995) 1547. https://doi.org/10.1021/cm00056a022
16 T. Katsumata, T. Nabae, K. Sasajima, and T. Matsuzawa: J. Cryst. Growth **183** (1998) 361. https://doi.org/10.1016/0168-583X(96)00031-6
17 D. Ravichandran, S. T. Johnson, S. Erdei, R. Roy, and W. B. White: Displays **19** (1999) 197. https://doi.org/10.1016/S0141-9382(98)00050-X
18 H. Yamamoto and T. Matsuzawa: J. Lumin. **72–74** (1997) 287. https://doi.org/10.1016/S0022-2313(97)00012-4
19 C. Zhao and D. Chen: Mater. Lett. **61** (2007) 3673. https://doi.org/10.1016/j.matlet.2006.12.015
20 T. Aitasalo, J. Hölsä, H. Jungner, M. Lastusaari, J. Niittykoski, M. Parkkinen, and R. Valtonen: Opt. Mater. **26** (2004) 113. https://doi.org/10.1016/j.optmat.2003.11.007
21 T. Aitasalo, A. Durygin, J. Hölsä, M. Lastusaari, J. Niittykoski, and A. Suchocki: J. Alloys Compd. **380** (2004) 4. https://doi.org/10.1016/j.jallcom.2004.03.007
22 Y. H. Lin, M. Li, C. W. Nan, and Z. Zhang: J. Am. Ceram. Soc. **90** (2007) 2992. https://doi.org/10.1111/j.1551-2916.2007.01786.x
23 T. A. Devol, S. B. Chotoo, and R. A. Fjeld: Nucl. Instrum. Methods Phys. Res., Sect. A **425** (1999) 228. https://doi.org/10.1016/S0168-9002(98)01380-1
24 T. Yanagida, K. Kamada, Y. Fujimoto, H. Yagi, and T. Yanagitani: Opt. Mater. **35** (2013) 2480. https://doi.org/10.1016/j.optmat.2013.07.002
25 T. Yanagida, Y. Fujimoto, T. Ito, K. Uchiyama, and K. Mori: Appl. Phys. Express **7** (2014) 062401. https://doi.org/10.7567/APEX.7.062401
26 S. Tanabe, S. Todoroki, K. Hirao, and N. Soga: J. Non-Cryst. Solids **122** (1990) 59. https://doi.org/10.1016/0022-3093(90)90225-B
27 S. H. M. Poort, A. Meyerink, and G. Blasse: J. Phys. Chem. Solids **58** (1997) 1451. https://doi.org/10.1016/S0022-3697(97)00010-3
28 Y. Hasegawa, Y. Wada, S. Yanagida, H. Kawai, N. Yasuda, and T. Nagamura: Appl. Phys. Lett. **83** (2003) 3599. https://doi.org/10.1063/1.1616207
29 D. Nakauchi, G. Okada, and T. Yanagida: J. Ceram. Soc. Jpn. **124** (2016) 546. https://doi.org/10.2109/jcersj2.15232
30 E. Sakai: IEEE Trans. Nucl. Sci. **34** (1987) 418. https://doi.org/10.1109/TNS.1987.4337375
31 T. Toizumi, S. Inagawa, T. Nakamori, J. Kataoka, Y. Tsubuku, Y. Yatsu, T. Shimokawabe, N. Kawai, T. Okada, and I. Ohtsu: Nucl. Instrum. Methods Phys. Res., Sect. A **604** (2009) 168. https://doi.org/10.1016/j.nima.2009.01.063